Cytokinin signaling alters acid-fast staining of *Mycobacterium tuberculosis*

Marie I. Samanovic[1], Hao-Chi Hsu[2], Marcus B. Jones[3], Victoria Jones[4], Michael R. McNeil[4], Samuel H. Becker[1], Susan Zhang[1], Ashley T. Jordan[1], Miroslav Strnad[5], Mary Jackson[4], Huilin Li[2]* and K. Heran Darwin[1]*

[1]Department of Microbiology, New York University School of Medicine, New York, NY 10016, USA

[2]The Van Andel Research Institute, Grand Rapids, MI 49503, USA

[3]Human Longevity, Inc., San Diego, CA 92121, USA

[4]Mycobacteria Research Laboratories, Department of Microbiology, Immunology and Pathology, Colorado State University, Fort Collins, CO 80523-1682, USA

[5]Laboratory of Growth Regulators, Centre of the Region Haná for Biotechnological and Agricultural Research, Institute of Experimental Botany ASCR and Palacký University, 78371 Olomouc, Czech Republic

Corresponding authors: heran.darwin@med.nyu.edu

Huilin.Li@vai.org

Keywords: *Mycobacterium tuberculosis*, cytokinins, cell envelope, proteasome, Pup, antibiotic resistance

Summary

It was recently reported the human-exclusive pathogen *Mycobacterium (M.) tuberculosis* secretes cytokinins, which had only been known as plant hormones. While cytokinins are well-established, adenine-based signaling molecules in plants, they have never been shown to participate in signal transduction in other kingdoms of life. *M. tuberculosis* is not known to interact with plants. Therefore we tested the hypothesis that cytokinins trigger transcriptional changes within this bacterial species. Here, we show cytokinins induced the strong expression of the *M. tuberculosis* gene, Rv0077c. We found that Rv0077c expression is repressed by a TetR-like transcriptional repressor, Rv0078. Strikingly, cytokinin-induced expression of Rv0077c resulted in a loss of acid-fast staining of *M. tuberculosis*. While acid-fast staining is thought to be associated with changes in the bacterial cell envelope and virulence, Rv0077c-induced loss of acid-fastness did not affect antibiotic susceptibility or attenuate bacterial growth in mice, consistent with an unaltered mycolic acid profile of Rv0077c-expressing cells. Collectively, these findings show cytokinins signal transcriptional changes that affect *M. tuberculosis* acid-fastness, and that cytokinin signaling is no longer limited to the kingdom plantae.

M. tuberculosis is the causative agent of tuberculosis, one of the world's leading causes of mortality[1]. For this reason, researchers are eager to identify pathways that could be targeted for the development of new therapeutics to treat this devastating disease. Among the current prioritized targets is the mycobacterial proteasome. *M. tuberculosis* strains with defects in proteasome-dependent degradation are highly attenuated in mice, partly because they are sensitive to nitric oxide (NO)[2-7]. We recently reported that the NO-sensitive phenotype of a mutant defective for proteasomal degradation is due to an inability to degrade an enzyme called Log (Lonely guy), a homologue of plant enzymes involved in the biosynthesis of cytokinins, which are N^6-substituted adenine-based molecules[8]. The accumulation of Log in *M. tuberculosis* results in a buildup of cytokinins, which break down into adenine and aldehydes that sensitize mycobacteria to NO[8].

Cytokinins are hormones that regulate the growth and development of plants[9]. In addition, bacterial plant pathogens and symbionts use cytokinins to facilitate the parasitism of plants[10]. Our prior study was the first to identify a mammalian pathogen that secretes cytokinins. Outside of the laboratory, *M. tuberculosis* exclusively infects humans and is not known to have an environmental reservoir; therefore, it is unlikely *M. tuberculosis* secretes cytokinins to modulate plant development. Instead, we hypothesized *M. tuberculosis* uses cytokinins to signal intra-species transcriptional changes like plants. To test this hypothesis, we grew wild type (WT) *M. tuberculosis* H37Rv (Supplementary Table 1) to mid-logarithmic phase and incubated the bacteria for five hours with N^6-(Δ^2-isopentenyl)adenine (iP), one of the most abundantly produced cytokinins in *M. tuberculosis* that is also commercially available[8]. Using RNA-

Seq, we discovered the expression of four genes, Rv0076c, Rv0077c, Rv0078, and *mmpL6*, was significantly induced upon iP treatment compared to treatment with the vehicle control (dimethylsulfoxide, DMSO) (Supplementary Table 2, Supplementary Fig. 1a, b). Rv0077c is conserved among many mycobacterial species, while Rv0076c and Rv0078 are present only in several mycobacterial genomes (Supplementary Fig. 1c)[11]. *M. smegmatis*, a distant, non-pathogenic relative of *M. tuberculosis*, has a weak homologue of Rv0077c and no conspicuous Rv0078 homologue (Supplementary Fig. 1c). *mmpL6* is one of 13 *mmpL* (mycobacterial membrane protein large) genes in *M. tuberculosis*. In strain H37Rv, *mmpL6* is predicted to encode a 42 kD protein with five trans-membrane-domains and is truncated compared to the same gene in ancestral tuberculosis strains[12]. Thus, it is unclear if *mmpL6* encodes a functional protein in strain H37Rv.

We raised polyclonal antibodies to recombinant Rv0077c protein and showed that protein levels were increased in *M. tuberculosis* treated with iP for 24 hours (Fig. 1a). Rv0077c was barely detectable in cell lysates of bacteria that had not been incubated with iP and was undetectable in a strain that has a transposon insertion mutation in Rv0077c (Fig. 1a). Rv0077c protein was restored to WT levels in the mutant upon complementation with an integrative plasmid encoding Rv0077c expressed from its native promoter (Fig. 1a). We also found a dose-dependent induction of Rv0077c production using iP concentrations from 1 nM to 100 μM (Fig. 1b).

We next synthesized and tested if the most abundantly produced cytokinin in *M. tuberculosis*, 2-methyl-thio-iP (2MeSiP)[8], could also induce Rv0077c production. 2MeSiP strongly induced Rv0077c production (Fig. 1c, lane 4). Importantly, we did not

observe induction of Rv0077c when we incubated the bacteria with the appropriate cytokinin riboside (R) precursors iPR or 2MeSiPR (Fig. 1c, lanes 3 and 5). Similarly, the closely related molecules adenine or adenosine monophosphate (AMP) could not induce Rv0077c synthesis (Fig. 1c, lanes 6 and 7).

The base structure of all cytokinins is adenine. We hypothesized while adenine could not induce Rv0077c expression, at high enough concentrations it could possibly inhibit Rv0077c induction by competing with iP for access to a transporter or receptor. Indeed, adenine reduced the induction of Rv0077c by iP in a dose-dependent manner (Fig. 1d).

In order to understand the consequences of cytokinin gene induction in *M. tuberculosis*, we sought to determine the function of Rv0077c. In the absence of cytokinin, Rv0077c is not expressed well under normal culture conditions; therefore, we sought to make a mutant that constitutively expressed Rv0077c in order to understand its function. Rv0077c is divergently expressed from Rv0078 (Supplementary Fig. 1b), which encodes a putative TetR-like transcriptional regulator; the proposed translational start codons for these genes are separated by 61 base pairs therefore we hypothesized that Rv0078 encodes a repressor of Rv0077c expression. We identified the promoters for each gene by performing rapid amplification of 5’ complementary DNA ends (5'RACE) analysis for Rv0077c and Rv0078 and determined the start of transcription for each gene is encoded within the 5' untranslated region of the other gene (Fig. 2a). Furthermore, using an electrophoretic mobility shift assay (EMSA, Fig. 2b) we narrowed down the putative Rv0078 binding site to a palindrome overlapping the starts of transcription of both Rv0077c and Rv0078 (Fig. 2a, red box). Substitutions in the

putative binding site prevented the binding of Rv0078 to the DNA probes (Fig. 2b). Notably, the addition of the cytokinin iP did not result in the release of Rv0078 from the probe (Supplementary Fig. 2) therefore it does not appear that cytokinins directly bind to Rv0078 to induce gene expression.

Based on the 5'RACE analysis we were able to delete and replace most of the Rv0078 gene with the hygromycin-resistance gene (*hyg*) without disrupting the promoter of Rv0077c from *M. tuberculosis* H37Rv. The ΔRv0078::*hyg* strain displayed constitutively high expression of Rv0077c irrespective of the presence of cytokinin, supporting a model where Rv0078 directly represses Rv0077c expression (Fig. 2c). A single copy of Rv0078 expressed from its native promoter restored iP-regulated control of Rv0077c in this strain (Fig. 2c, lanes 5 and 6). Interestingly, in the process of making the complementation plasmid for Rv0078, we acquired a PCR-generated, random mutation in Rv0078 that changed a tryptophan to arginine (W100R). Expression of this allele was unable to complement the Rv0078 deletion (Fig. 2c, lanes 7 and 8).

We solved the crystal structure of *M. tuberculosis* Rv0078 purified from *Escherichia coli* to 1.85 Å resolution (Fig. 2d,e; Supplementary Table 3). Rv0078 formed a dimer with a fold highly similar to the TetR repressor and its family members[13]. Helices α1 to α3 form the DNA binding domain (DBD), while helices α4 to α9 constitute an elongated ligand-binding domain (LBD) (Fig. 2d). The distance between the two DNA-binding α3 helices of the protomers is 42 Å, which is comparable to the distances of 35 - 38 Å of other TetR family proteins[13,14] Interestingly, we found that W100, faces the LBD (Fig. 2e), which may explain why the $Rv0078_{W100R}$ mutant allele was unable restore cytokinin-dependent regulation to the Rv0078 mutant strain (Fig. 2c, lane 8).

During our studies, a report was published on the identification of a small molecule of the spiroisoxazoline family, SMARt-420, which strongly induces the expression of the Rv0077c orthologue *bcg_0108c* in *M. bovis* Bacille Calmette-Guerin[15]. Using x-ray crystallography and surface plasmon resonance techniques, the authors of this study found SMARt-420 binds to Rv0078 to derepress binding from the Rv0077c promoter[15,16]. SMARt-420 was identified in a search for compounds that could boost the efficacy of the second-line tuberculosis drug ethionamide (ETH). ETH is a pro-drug that is activated by the mono-oxygenase EthA, which transforms ETH into highly reactive intermediates. Activated ETH and nicotinamide adenine dinucleotide form a stable adduct, which binds to and inhibits InhA, an essential enzyme needed for mycolic acid synthesis in mycobacteria[17,18]. While spontaneous inactivating mutations in *ethA* can result in resistance to ETH, it was proposed that the induction of Rv0077c expression could bypass the need for EthA and transform ETH into its toxic form[15]. Based on this study, we predicted that an Rv0078 mutant of *M. tuberculosis*, which expresses high levels of Rv0077c (Fig. 2c, lanes 3 and 4), should be hypersensitive to ETH compared to the parental strain H37Rv. However, we observed either little to no significant change in the 50% minimum inhibitory concentration (MIC_{50}) of ETH between the WT and ΔRv0078::*hyg* strains (Supplementary Table 4). It is possible that the effects of SMARt-402 is growth-condition dependent, that this molecule affects another pathway to either increase the susceptibility of *M. tuberculosis* to ETH, or that another SMARt-420-induced enzyme in addition to Rv0077c synergize together to activate ETH (A. Baulard, personal communication).

We also tested if the constitutive expression of Rv0077c changed the susceptibility of *M. tuberculosis* to other antibiotics, including two cell wall synthesis inhibitors. We observed no differences in the MIC_{50} of these antibiotics between the WT and ΔRv0078::*hyg* strains (Supplementary Table 4).

To gain insight into the function of the most strongly cytokinin-induced gene Rv0077c, we prepared total cell lysate samples of WT and Rv0077c mutant strains treated with 100 μM iP for 24 hours for metabolomic analysis. From a total of 337 detectable metabolites, we observed a significant change in 24 molecules after the addition of iP to WT *M. tuberculosis*. Importantly, 17 metabolites showed a consistent difference between samples in which Rv0077c was produced and these changes disappeared in an Rv0077c-disrupted strain, suggesting the changes observed in iP-treated WT *M. tuberculosis* were specifically due to the presence of Rv0077c (Supplementary Table 5, highlighted in yellow). We observed an increased abundance of several phospholipids and a decrease in a major precursor of peptidoglycan, N-acetyl-glucosamine-1-phosphate (GlcNAc1P). We therefore hypothesized that Rv0077c modified one or more components of the cell envelope. Microscopic examination of Ziehl-Neelsen stained WT *M. tuberculosis* treated with iP showed a dramatic loss of acid-fast staining (Fig. 3, panel a compared to b), and this phenotype depended on the presence of Rv0077c (Fig. 3, panel c compared to d). Complementation of the mutation with Rv0077c alone restored the iP-induced loss of acid-fast staining (Fig. 3, panels e and f). Deletion of Rv0078 resulted in the constitutive loss of acid-fast staining, irrespective of the presence of iP (Fig. 3, panels g and h). Complementation of the Rv0078 deletion with the WT gene restored iP-control of loss acid-fast staining (Fig. 3,

panels i and j) but complementation with Rv0078$_{W100R}$, which could not fully de-repress Rv0077c expression in the presence of iP (Fig. 2c), could not restore iP-induced loss of acid-fast staining (Fig. 3, panels k and l). Mixing and thus simultaneous staining of the Rv0077c and Rv0078 mutants further showed the staining differences were not a result of a technical artifact (Fig. 3m).

Acid-fast staining is thought to be associated with mycolic acids; alterations in mycolic acid synthesis results in negative effects on cell growth *in vitro* and *in vivo*[19,20]. We used thin layer and liquid or gas chromatography coupled to mass spectrometry to analyze the fatty acid, mycolic acid and lipid contents of the WT, Rv0077c and Rv0078 strains and observed no significant qualitative or quantitative differences between strains (Supplementary Fig. 3 and Supplementary Table 6). In particular, the expression of Rv0077c did not conspicuously modify the chain length of mycolic acids, their cyclopropanation or the relative abundance of keto- to alpha- mycolates, and did not alter the wax ester and triglyceride content of the strains that have been previously been linked to acid-fast staining[20,21]. These results are consistent with the observed lack of defects in growth and drug susceptibility *in vitro*.

Finally, we tested if either the Rv0077c or Rv0078 mutant had growth defects *in vivo* compared to the WT H37Rv strain. We infected C57BL/6J mice by a low-dose aerosol route with the parental, mutant, and complemented mutant strains, as well as with the Rv0078 mutant transformed with the Rv0078$_{W100R}$ mutant allele. Interestingly, none of the strains revealed a difference in growth or survival compared to WT *M. tuberculosis* in mice as determined by the recovery of colony forming units (CFU) from the lungs and spleens (Fig. 4 and Supplementary Fig. 4). While we did not observe any

differences in bacterial burden in mice infected with the *log*[8], Rv0077c or Rv0078 mutants, it is possible that Rv0077c function might only be needed during late stages of infection, an idea that is supported by a previous observation that the *log* homologue needed for cytokinin synthesis in *M. marinum* is specifically expressed in late granulomas of infected frogs[22]. Furthermore, mice might not provide the optimal model to observe a role for these proteins in tuberculosis.

Taken together, this is the first study to demonstrate that cytokinins induce transcriptional and physiologic changes in bacteria. In plants, defects in cytokinin signaling can result in profound developmental problems, such as abnormal root and flower development[23]. While we observed dramatic changes in the ability of cytokinin-treated *M. tuberculosis* to retain stain, we did not observe a significant impact on virulence in mice. Nonetheless, ongoing studies will elucidate the cytokinin signal transduction pathway and the natural target of Rv0077c, the understanding of which may provide new insight into the elusive molecular basis of acid-fastness of this human-exclusive pathogen. Rv0077c is predicted to have an α/β hydrolase fold[24], which we hypothesize may target one or more components of the cell envelope. Loss of acid fast staining of *M. tuberculosis* in human and mouse tissues over time has been previously reported and presumed to be important for pathogenesis[25,26]. An important revelation during our studies was the inability of *M. tuberculosis* to stain with an acid-fast dye did not necessarily affect pathogenesis in a mouse infection model. This result may also indicate that acid fast staining is affected by different mechanisms. It also remains to be determined what the natural ligand is for the Rv0078 repressor; while SMARt-420 binds robustly to Rv0078[15,16] the cytokinin iP did not. This result is consistent with the

observation that SMARt-420 and cytokinins bear no resemblance to each other. Finally, our studies have opened the door to the possibility that numerous commensal and pathogenic microbes (including fungi) could use cytokinins for intra- or inter-species communication in complex systems such as the gut microbiome.

Author Contributions M.I.S. and K.H.D. performed *in vitro* and *in vivo M. tuberculosis* work. M.B.J. performed the RNA-Seq analysis. H.C.H. and H.L. determined the structure of Rv0078 and performed the EMSA assays. S.H.B. and A.T.J. performed antibiotic susceptibility assays. S.Z. assisted with the mouse experiments. V.J., M.R.M. and M.J. performed the lipid analysis. M.S. synthesized cytokinins and their precursors. M.I.S. and K.H.D. wrote the manuscript.

Acknowledgments We thank A. Darwin and V. Torres for critical review of a draft version of this manuscript. This work was supported by NIH grant R01HL092774 awarded to K.H.D. K.H.D. holds an Investigators in the Pathogenesis of Infectious Disease Award from the Burroughs Wellcome Fund. M.I.S. and S.H.B were supported by the Jan T. Vilcek Endowed Fellowship fund. S.H.B. is also supported by NIH grant T32 AT007180. H.C.H. and H.L. were supported by R01AI070285. M. Strnad was supported by LO1204 from the National Program of Sustainability I. We thank A. Liang and Y. Deng of the Microscopy Laboratory at New York University Langone Medical Center for assistance with microscopy and imaging. Diffraction data for this study were collected at the Lilly Research Laboratories Collaborative Access Team (LRL-CAT) beamline at the Advanced Photon Source (APS), Argonne National Laboratory. APS

was supported by the U.S. Department of Energy, Office of Science, Office of Basic Energy Sciences, under Contract DE-AC02-06CH11357. Use of the LRL-CAT beamline at Sector 31 of the APS was provided by Eli Lilly Co., which operates the facility.

Methods

Bacterial strains, plasmids, primers, chemicals, and culture conditions. Bacterial strains, plasmids, and primer sequences used in this study are listed in Supplementary Table 1. All primers for cloning and sequencing were from Invitrogen, Inc. *M. tuberculosis* strains were grown in Middlebrook 7H9 broth (Difco) supplemented with 0.2% glycerol, 0.05% Tween-80, 0.5% fraction V bovine serum albumin, 0.2% dextrose and 0.085% sodium chloride ("7H9c"). *M. tuberculosis* cultures were grown without shaking in 25 or 75 cm^2 vented flasks (Corning) at 37ºC. 7H11 agar (Difco) supplemented with 0.5% glycerol and BBL TM Middlebrook OADC enrichment (BD) was used for growth on solid medium ("7H11"). *M. tuberculosis* was transformed as described[27]. *E. coli* strains used for cloning and expression were grown in LB-Miller broth (Difco) at 37°C with aeration on a shaker or on LB agar. *E. coli* strains were chemically transformed as previously described[28]. The final concentrations of antibiotics used for *M. tuberculosis* growth: kanamycin, 50 µg/ml; hygromycin, 50 µg/ml; streptomycin, 25 µg/ml; and for *E. coli*: hygromycin, 150 µg/ml; kanamycin, 100 µg/ml; and streptomycin 50 µg/ml. AMP, adenine and iP were purchased from Sigma. iPR, 2MeSiP and 2MeSiPR were synthesized as previously described[29]. The purity of the synthesized cytokinin and derivatives was >98% for each as determined by high performance liquid chromatography and mass spectrometry.

The Rv0077c::MycoMarT7 mutant was isolated from a library of ordered transposon insertion mutants as previously described[3,30]. The ΔRv0078::*hyg* mutant was made by deletion-disruption mutagenesis as described in detail elsewhere using pYUB854[31].

Protein purification and immunoblotting. DNA sequence encompassing the full-length Rv0078 or Rv0077c gene was cloned into pET24b(+) vector using primers listed in Supplementary Table S1. Recombinant proteins were produced in *E. coli* ER2566 and purified under native conditions for Rv0078 and denaturing conditions for Rv0077c according to the manufacturer's specifications (Qiagen). Polyclonal rabbit antibodies were raised by Covance (Denver, PA). For all immunoblots, cell lysates or purified proteins were separated sodium dodecyl sulfate polyacrylamide gel electrophoresis (SDS-PAGE); transferred to nitrocellulose and incubated with rabbit polyclonal antibodies to the protein of interest at 1:1000 dilution in 3% bovine serum albumin in TBST (25 mM Tris-HCl, pH 7.4, 125 mM NaCl, 0.05% Tween 20, pH 7.4). Equal loading was determined by stripping the nitrocellulose membranes with 0.2 N NaOH for 5 min, rinsing, blocking and incubating the nitrocellulose with polyclonal rabbit antibodies to dihydrolipoamide acyltransferase (DlaT)[32]. Horseradish peroxidase conjugated anti-rabbit antibody (GE-Amersham Biosciences) was used for chemiluminescent detection (SuperSignal West Pico; ThermoScientific).

For crystallography studies of Rv0078-His_6, bacteria were grown at 37°C to an OD_{600} = 0.5-0.6 before being induced with 0.5 mM IPTG and incubated at 16°C overnight. After harvesting by centrifugation, cells were lysed by passing through a

microfluidizer cell disruptor in 10 mM potassium phosphate, pH 8.0, 10 mM imidazole, and 500 mM NaCl. The homogenate was clarified by spinning at 27,000 *g* and the supernatant was applied to a HiTrap-Ni column (GE Healthcare) pre-equilibrated with the lysis buffer. Histidine-tagged protein was eluted with a 10–300 mM imidazole gradient in 10 mM potassium phosphate, pH 8.0, containing 300 mM M NaCl. The Rv0078 fractions were further purified by applying to a Superdex 75 column (16 x 1000 mm, GE Healthcare) pre-equilibrated with 20 mM potassium phosphate, pH 8.0, and 300 mM NaCl. For crystallization, the purified Rv0078 was concentrated to 40 mg/ml.

After solving the Rv0078 structure, we noticed that a strong density occupied the pocket near Glu70 and Trp100, which corresponds to the ligand-binding pocket of the TetR family proteins. Before performing the DNA binding assays, we removed the unknown ligands by denaturing and refolding the protein. Briefly, the Rv0078 producing bacteria were lysed by sonication on ice in 100 mM potassium phosphate, pH 8.0, 10 mM imidazole, 500 mM NaCl, and 6 M guanidine hydrochloride. The homogenate was clarified by spinning at 27,000 *g* and the supernatant was applied to a HiTrap-Ni column pre-equilibrated with the lysis buffer. After washing with 10 column volumes of lysis buffer, proteins bound to the beads in column were refolded by using a 200 ml linear gradient from 6.0 M to 0.0 M guanidine hydrochloride in a buffer containing 10 mM potassium phosphate, pH 8.0, 10 mM imidazole, and 500 mM NaCl, at a flow rate of 0.2 ml/min. The refolded protein was subsequently eluted with a 10 - 500 mM imidazole gradient. The estimated molecular weight of refolded Rv0078 was similar to the native protein based on the elution volume in gel filtration columns.

Crystallization and structure determination. Crystals of the Rv0078-His_6 protein were obtained by screening at 293°K using sitting-drop vapor diffusion method. The C2 space group crystals were grown in 0.1 M sodium cacodylate, pH 6.4, and 1.3 M lithium sulfate. SeMet substituted Rv0078 crystals in C2 space group were grown in 0.1 M sodium cacodylate, pH 6.6, 1.3 M Lithium sulfate, 0.2 M magnesium sulfate, and 2% PEG400. Diffraction data to a resolution of 1.85 Å (native crystals) and 2.7 Å (Se-Met crystals) were collected at the Lilly Research Laboratories Collaborative Access Team (LRL-CAT) beamline of Advanced Photon Source (APS), Argonne National Laboratory, and were processed with Mosflm software. The program Hybrid Substructure Search of the Phenix package was used to locate the Se sites and initial phasing was carried out using Autosol of Phenix. The 2.7 Å map phased by SAD method allowed us to build atomic model unambiguously. The native Rv0078 structure was subsequently determined by the program PHASER using SeMet substituted Rv0078 as the initial search model. All of the refinements were performed using Phenix-refine[33] and the statistics were provided in Supplementary Table 3.

Metabolomic analysis of *M. tuberculosis* cell lysates. Four independent cultures of each analyzed strain were grown in 7H9 to an OD_{580} ~0.7 and treated with iP in DMSO at a final concentration of 100 μM or an equal volume of DMSO for 24 hours. Bacteria were harvested the next day at OD_{580} ~1. Sixty-five OD-equivalents per replicate were processed by chloroform:methanol extraction[8,34]. Metabolomic profiling was performed by Metabolon, Inc.

EMSA. A series of double stranded DNA probes consisting of sequences in the intergenic region between Rv0077c and Rv0078 were generated by annealing two complementary oligonucleotides and a 5'-end IRDye700-labeled 14-nucleotide oligomers (Integrated DNA Technologies). Binding assays were performed by incubating 100 nM of probes and various concentrations of Rv0078 at room temperature for 30 min in 20 mM HEPES, pH 7.5, 3 mM DTT, 0.1 mM EDTA, 100 mM KCl, 5% glycerol, 5 mg/ml BSA, 10 mM $MgCl_2$, and 0.25% Tween 20, and were subsequently resolved in 6% polyacrylamide gels (Bio-Rad) in 0.5 × TBE buffer. Mobility shifts of protein-DNA complex were visualized in LI-COR Odyssey imager.

RNA-Seq and 5'RACE. Three biological replicate cultures of WT *M. tuberculosis* were grown to an OD_{580} ~1 and incubated in 100 μM iP or DMSO (control) for five hours. Cells were harvested and RNA was purified as described previously [31]. Briefly, an equal volume of 4 M guanidinium isothiocyanate, 0.5% sodium N-lauryl sarcosine, 25 mM trisodium citrate solution was added to cultures to arrest transcription. RNA was isolated with Trizol Reagent (Invitrogen) and further purified using RNeasy Miniprep kits and DNase I (Qiagen). Transcriptome profiling by RNA-seq was performed and analyzed as follows: RNA from *M. tuberculosis* cultures were extracted for library construction. Libraries were constructed and barcoded with the Epicentre ScriptSeq Complete Gold low input (Illumina, Inc) and sequenced on Illumina HiSeq 2000 sequencer using version 3 reagents. Unique sequence reads were mapped to the corresponding reference genome and RPKM values were calculated in CLC (CLC version 7.0.4).

Genes with significantly different RPKM values were identified using the Significant Analysis for Microarray (SAM) statistical analysis component of MeV[35].

5'RACE was performed as described by the manufacturer (Invitrogen). Briefly, 1 µg of RNA was used as template for cDNA production using a reverse primer 150–300 bp downstream of annotated translational start sites. A 3' poly-C tail was added to cDNA by recombinant Tdt. The cDNA was then amplified using a nested reverse primer and a primer that anneals to the poly-C tail. Products were cloned and sequenced. Likely transcriptional start sites were selected based on clones that had the most nucleotide sequence upstream of the start codon.

Acid-fast staining and microscopy. *M. tuberculosis* strains were grown to mid-logarithmic phase (OD_{580} ~0.5-0.7). 5 µl of culture was spotted onto glass slides and heat-killed over a flame or on a heat block (15 min, 80˚C). Staining was performed according the method of Ziehl-Neelson as per the manufacturer's instructions (BD Stain Kit ZN). Images were acquired on a Zeiss Axio Observer with a Plan-Aprochromat 63x/1.4 oil lens. Images were taken with an Axiocam503 camera at the NYULMC Microscopy Laboratory.

Analysis of total lipids, mycolic acids and shorter chain fatty acids. For lipid analysis 400 ml cultures were grown up to OD_{580} ~0.7 and treated with iP in DMSO at a final concentration of 100 µM or an equal volume of DMSO-only for 24 hours. 400 ml of Rv0077c and Rv0078 cultures were treated with DMSO only. Cells were washed three times in DPBS and heated at 100°C for 45 min for sterilization before freezing at -20 °C.

Total lipids extraction from bacterial cells and preparation of fatty acid and mycolic acid methyl esters from extractable lipids and delipidated cells followed earlier procedures [36]. Total lipids and fatty acid/mycolic acid methyl esters were analyzed by one and two-dimensional thin-layer chromatography (TLC) in a variety of solvent systems on aluminum-backed silica gel 60-precoated plates F_{254} (E. Merck). TLC plates were revealed by spraying with cupric sulfate (10% in a 8% phosphoric acid solution) and heating. Alternatively, total lipids were run in both positive and negative mode and the released fatty acids/mycolic acids in negative mode only, on a high resolution Agilent 6220 TOF mass spectrometer interfaced to a LC as described[37,38]. Data files were analyzed with Agilent's Mass hunter work station software and most compounds were identified using a database of *M. tuberculosis* lipids developed in-house [37]. Fatty acids methyl esters from extractable lipids were treated with 3 M HCl in CH_3OH (Supelco) overnight at 80˚C, dried and dissolved in *n*-hexane(s) prior to GC/MS analysis. GC/MS analyses of fatty acid methyl esters were carried out using a TRACE 1310 gas chromatograph (Thermo Fisher) equipped with a TSQ 8000 Evo Triple Quadrupole in the electron impact mode and scanning from *m/z* 70 to *m/z* 1000 over 0.8 s. Helium was used as the carrier gas with a flow rate of 1 ml per min. The samples were run on a ZB-5HT column (15 m x 0.25 mm i.d.) (Zebron). The injector (splitless mode) was set for 300°C (350°C for mycolic acid methyl esters). The oven temperature was held at 60°C for 2 min, programmed at 20°C per min to 375°C, followed by a 10 min hold. The data analyses were carried out on Chromeleon data station.

MIC_{50} Determination. To determine the MIC_{50} of each antibiotic, *M. tuberculosis* strains were grown to an OD_{580} ~0.7 and diluted into fresh media to an OD_{580} of 0.02. Diluted cultures were transferred to a 96-well microtiter plate containing triplicate, 10-fold serial dilutions of antibiotic. Cell wall-active antibiotics (vancomycin, meropenem) were supplemented at all concentrations with potassium clavalunate to inhibit the intrinsic β-lactamase activity of *M. tuberculosis*. After five days of incubation at 37ºC, growth of each strain was measured by OD_{580}. MIC_{50} values were interpolated from a non-linear least squares fit of log_2-transformed OD_{580} measurements. Data are representative of two independent experiments. Antibiotics were purchased from Sigma-Aldrich (clavulanate, ethionamide, meropenem, rifampicin, vancomycin) or Thermo-Fisher Scientific (ciprofloxacin, ethambutol, isoniazid, norfloxacin, streptomycin).

Mouse Infections. Mouse infections were performed essentially as described previously[3]. 7-9-week-old female C57BL6/J mice (The Jackson Laboratory) were infected by aerosol to deliver ~200 bacilli per mouse, using a Glas-Col Inhalation Exposure System (Terre Haute, IN). Strains used were WT (MHD761) or (MHD794), Rv0077c (MHD1086), Rv0077c complemented (MHD1077), Rv0078 (MHD1315), Rv0078 complemented with WT Rv0078 (MHD1318) and $Rv0078_{W100R}$ (MHD1316). Mice were humanely euthanized according to an approved Institutional Animal Care and Use Committee protocol. Lungs and spleens were harvested and homogenized PBS/0.05% Tween-80 at indicated time points to determine bacterial CFU.

Data availability. Authors can confirm that all relevant data are included in the paper and/or its supplementary information files or are available on request from the authors.

References

1 WHO. http://www.who.int/mediacentre/factsheets/fs104/en/. (2017).

2 Cerda-Maira, F. A. *et al.* Molecular analysis of the prokaryotic ubiquitin-like protein (Pup) conjugation pathway in Mycobacterium tuberculosis. *Mol Microbiol* **77**, 1123-1135, doi:MMI7276 [pii]10.1111/j.1365-2958.2010.07276.x (2010).

3 Darwin, K. H., Ehrt, S., Gutierrez-Ramos, J. C., Weich, N. & Nathan, C. F. The proteasome of Mycobacterium tuberculosis is required for resistance to nitric oxide. *Science* **302**, 1963-1966, doi:10.1126/science.1091176302/5652/1963 [pii] (2003).

4 Gandotra, S., Lebron, M. B. & Ehrt, S. The Mycobacterium tuberculosis proteasome active site threonine is essential for persistence yet dispensable for replication and resistance to nitric oxide. *PLoS Pathog* **6**, doi:10.1371/journal.ppat.1001040 (2010).

5 Gandotra, S., Schnappinger, D., Monteleone, M., Hillen, W. & Ehrt, S. In vivo gene silencing identifies the Mycobacterium tuberculosis proteasome as essential for the bacteria to persist in mice. *Nat Med* **13**, 1515-1520, doi:nm1683 [pii]10.1038/nm1683 (2007).

6 Lamichhane, G. *et al.* Deletion of a Mycobacterium tuberculosis proteasomal ATPase homologue gene produces a slow-growing strain that persists in host tissues. *J Infect Dis* **194**, 1233-1240, doi:JID36050 [pii]10.1086/508288 (2006).

7 Lin, G. *et al.* Inhibitors selective for mycobacterial versus human proteasomes. *Nature* **461**, 621-626, doi:10.1038/nature08357 (2009).

8 Samanovic, M. I. *et al.* Proteasomal control of cytokinin synthesis protects Mycobacterium tuberculosis against nitric oxide. *Mol Cell* **57**, 984-994, doi:10.1016/j.molcel.2015.01.024 (2015).

9 Sakakibara, H. Cytokinins: activity, biosynthesis, and translocation. *Annu Rev Plant Biol* **57**, 431-449, doi:10.1146/annurev.arplant.57.032905.105231 [doi] (2006).

10 Frebort, I., Kowalska, M., Hluska, T., Frebortova, J. & Galuszka, P. Evolution of cytokinin biosynthesis and degradation. *J Exp Bot* **62**, 2431-2452, doi:err004 [pii]10.1093/jxb/err004 (2011).

11 Lechat, P., Hummel, L., Rousseau, S. & Moszer, I. GenoList: an integrated environment for comparative analysis of microbial genomes. *Nucleic Acids Res* **36**, D469-474, doi:10.1093/nar/gkm1042 (2008).

12 Brosch, R. *et al.* A new evolutionary scenario for the Mycobacterium tuberculosis complex. *Proc Natl Acad Sci U S A* **99**, 3684-3689, doi:10.1073/pnas.052548299 (2002).
13 Orth, P., Schnappinger, D., Hillen, W., Saenger, W. & Hinrichs, W. Structural basis of gene regulation by the tetracycline inducible Tet repressor-operator system. *Nat Struct Biol* **7**, 215-219, doi:10.1038/73324 (2000).
14 Schumacher, M. A. *et al.* Structural basis for cooperative DNA binding by two dimers of the multidrug-binding protein QacR. *EMBO J* **21**, 1210-1218, doi:10.1093/emboj/21.5.1210 (2002).
15 Blondiaux, N. *et al.* Reversion of antibiotic resistance in Mycobacterium tuberculosis by spiroisoxazoline SMARt-420. *Science* **355**, 1206-1211, doi:10.1126/science.aag1006 (2017).
16 Wohlkonig, A. *et al.* Structural analysis of the interaction between spiroisoxazoline SMARt-420 and the Mycobacterium tuberculosis repressor EthR2. *Biochem Biophys Res Commun* **487**, 403-408, doi:10.1016/j.bbrc.2017.04.074 (2017).
17 DeBarber, A. E., Mdluli, K., Bosman, M., Bekker, L. G. & Barry, C. E., 3rd. Ethionamide activation and sensitivity in multidrug-resistant Mycobacterium tuberculosis. *Proc Natl Acad Sci U S A* **97**, 9677-9682 (2000).
18 Vannelli, T. A., Dykman, A. & Ortiz de Montellano, P. R. The antituberculosis drug ethionamide is activated by a flavoprotein monooxygenase. *J Biol Chem* **277**, 12824-12829, doi:10.1074/jbc.M110751200 (2002).
19 Barkan, D., Liu, Z., Sacchettini, J. C. & Glickman, M. S. Mycolic acid cyclopropanation is essential for viability, drug resistance, and cell wall integrity of Mycobacterium tuberculosis. *Chem Biol* **16**, 499-509, doi:10.1016/j.chembiol.2009.04.001 (2009).
20 Bhatt, A. *et al.* Deletion of kasB in Mycobacterium tuberculosis causes loss of acid-fastness and subclinical latent tuberculosis in immunocompetent mice. *Proc Natl Acad Sci U S A* **104**, 5157-5162, doi:10.1073/pnas.0608654104 (2007).
21 Deb, C. *et al.* A novel in vitro multiple-stress dormancy model for Mycobacterium tuberculosis generates a lipid-loaded, drug-tolerant, dormant pathogen. *PLoS One* **4**, e6077, doi:10.1371/journal.pone.0006077 (2009).
22 Ramakrishnan, L., Federspiel, N. A. & Falkow, S. Granuloma-specific expression of Mycobacterium virulence proteins from the glycine-rich PE-PGRS family. *Science* **288**, 1436-1439, doi:8504 [pii] (2000).
23 Hwang, I., Sheen, J. & Muller, B. Cytokinin signaling networks. *Annu Rev Plant Biol* **63**, 353-380, doi:10.1146/annurev-arplant-042811-105503 [doi] (2012).
24 Soding, J., Biegert, A. & Lupas, A. N. The HHpred interactive server for protein homology detection and structure prediction. *Nucleic Acids Res* **33**, W244-248, doi:10.1093/nar/gki408 (2005).
25 Seiler, P. *et al.* Cell-wall alterations as an attribute of Mycobacterium tuberculosis in latent infection. *J Infect Dis* **188**, 1326-1331, doi:10.1086/378563 (2003).
26 Canetti, G. *The Tubercle Bacillus: The Pulmonary Lesion of Man*. (Springer Publishing Company, Inc., 1955).
27 Hatfull, G. F. & Jacobs, W. R. J. *Molecular Genetics of Mycobacteria*. (ASM Press, Washington, DC, 2000).

28 Sambrook, J., Maniatis, T. & Fritsch, E. *Molecular Cloning: A Laboratory Manual.* . (Cold Spring Harbor: Cold Spring Harbor Laboratory Press., 1989).
29 Sugiyama, T. & Hashizume, T. Ribosylation of 6-Chloropurine and Its 2 Methylthio Derivative by a Fusion Procedure Using Iodin. *Agric. Biol. Chem.* **42**, 1791-1792 (1978).
30 Festa, R. A., Pearce, M. J. & Darwin, K. H. Characterization of the proteasome accessory factor (paf) operon in Mycobacterium tuberculosis. *J Bacteriol* **189**, 3044-3050, doi:JB.01597-06 [pii]10.1128/JB.01597-06 (2007).
31 Festa, R. A. *et al.* A novel copper-responsive regulon in Mycobacterium tuberculosis. *Mol Microbiol* **79**, 133-148, doi:10.1111/j.1365-2958.2010.07431.x (2011).
32 Tian, J. *et al.* Mycobacterium tuberculosis appears to lack alpha-ketoglutarate dehydrogenase and encodes pyruvate dehydrogenase in widely separated genes. *Mol Microbiol* **57**, 859-868, doi:10.1111/j.1365-2958.2005.04741.x (2005).
33 Adams, P. D. *et al.* PHENIX: a comprehensive Python-based system for macromolecular structure solution. *Acta Crystallogr D Biol Crystallogr* **66**, 213-221, doi:10.1107/S0907444909052925 (2010).
34 Layre, E. *et al.* A comparative lipidomics platform for chemotaxonomic analysis of Mycobacterium tuberculosis. *Chem Biol* **18**, 1537-1549, doi:10.1016/j.chembiol.2011.10.013 (2011).
35 Saeed, A. I. *et al.* TM4: a free, open-source system for microarray data management and analysis. *Biotechniques* **34**, 374-378 (2003).
36 Stadthagen, G. *et al.* p-Hydroxybenzoic acid synthesis in Mycobacterium tuberculosis. *J Biol Chem* **280**, 40699-40706, doi:10.1074/jbc.M508332200 (2005).
37 Sartain, M. J., Dick, D. L., Rithner, C. D., Crick, D. C. & Belisle, J. T. Lipidomic analyses of Mycobacterium tuberculosis based on accurate mass measurements and the novel "Mtb LipidDB". *J Lipid Res* **52**, 861-872, doi:10.1194/jlr.M010363 (2011).
38 Bhamidi, S. *et al.* A bioanalytical method to determine the cell wall composition of Mycobacterium tuberculosis grown in vivo. *Anal Biochem* **421**, 240-249, doi:10.1016/j.ab.2011.10.046 (2012).

Samanovic et al, Figure 1

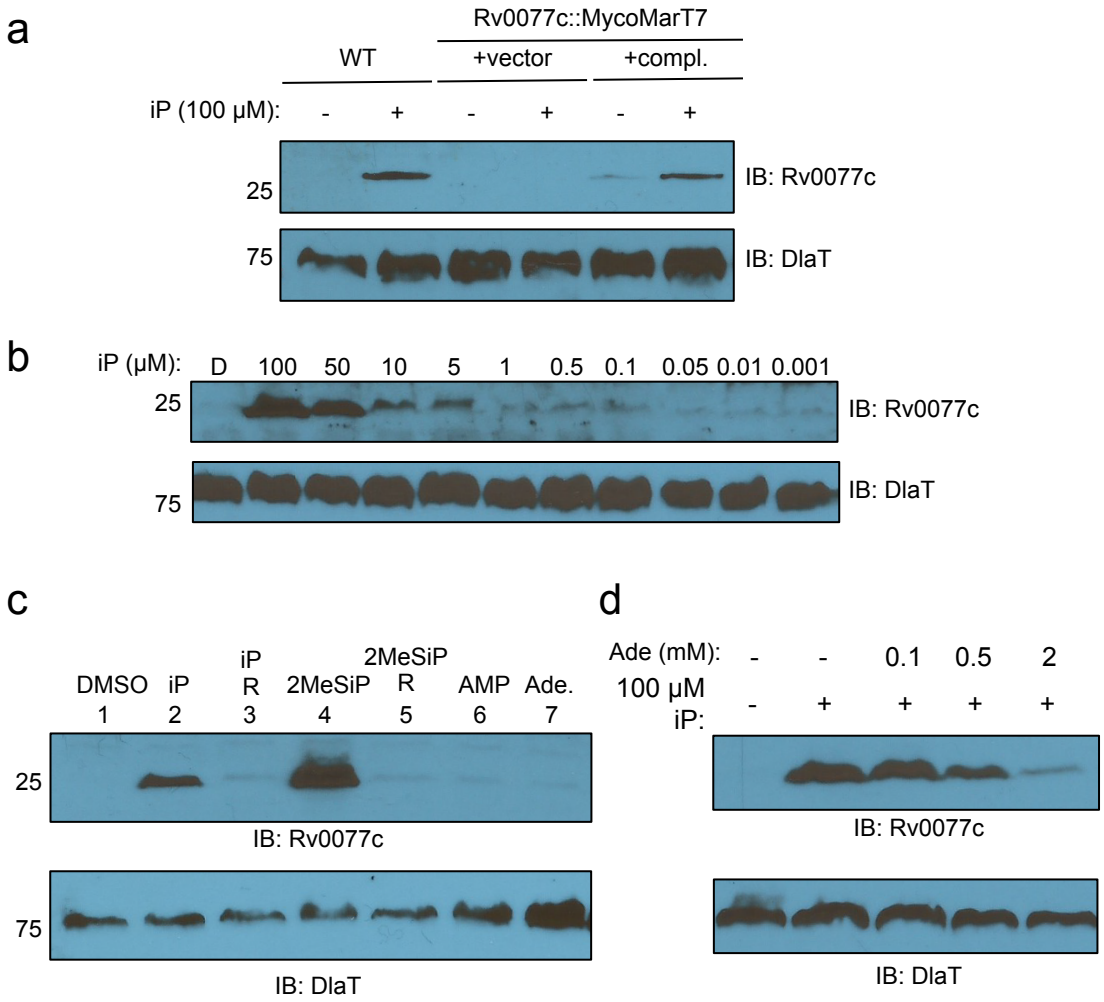

Figure 1. Cytokinins induce expression of Rv0077c in *M. tuberculosis*.
a, Immunoblot for Rv0077c in total cell lysates of WT *M. tuberculosis*. "compl." = complemented. **b,** Dose-dependent production of Rv0077c protein. Bacteria were incubated with cytokinin at the indicated concentrations for 24 hours. **c,** Only cytokinins, and not closely related molecules, induce the production of Rv0077c. Each compound was added to a final concentration of 100 μM. "R" indicates the riboside form of the preceding indicated cytokinin. **d,** Adenine inhibits the induction of Rv0077c by iP. For all panels, we added an equal volume of DMSO where iP was not added. For all immunoblots (IB), we stripped the membranes and incubated them with antibodies to dihydrolipoamide acyltransferase (DlaT) to confirm equal loading of samples. Molecular weight standards are indicated to the left of the blots and are in kilodaltons (kD). Ade, adenine.

Samanovic et al, Figure 2

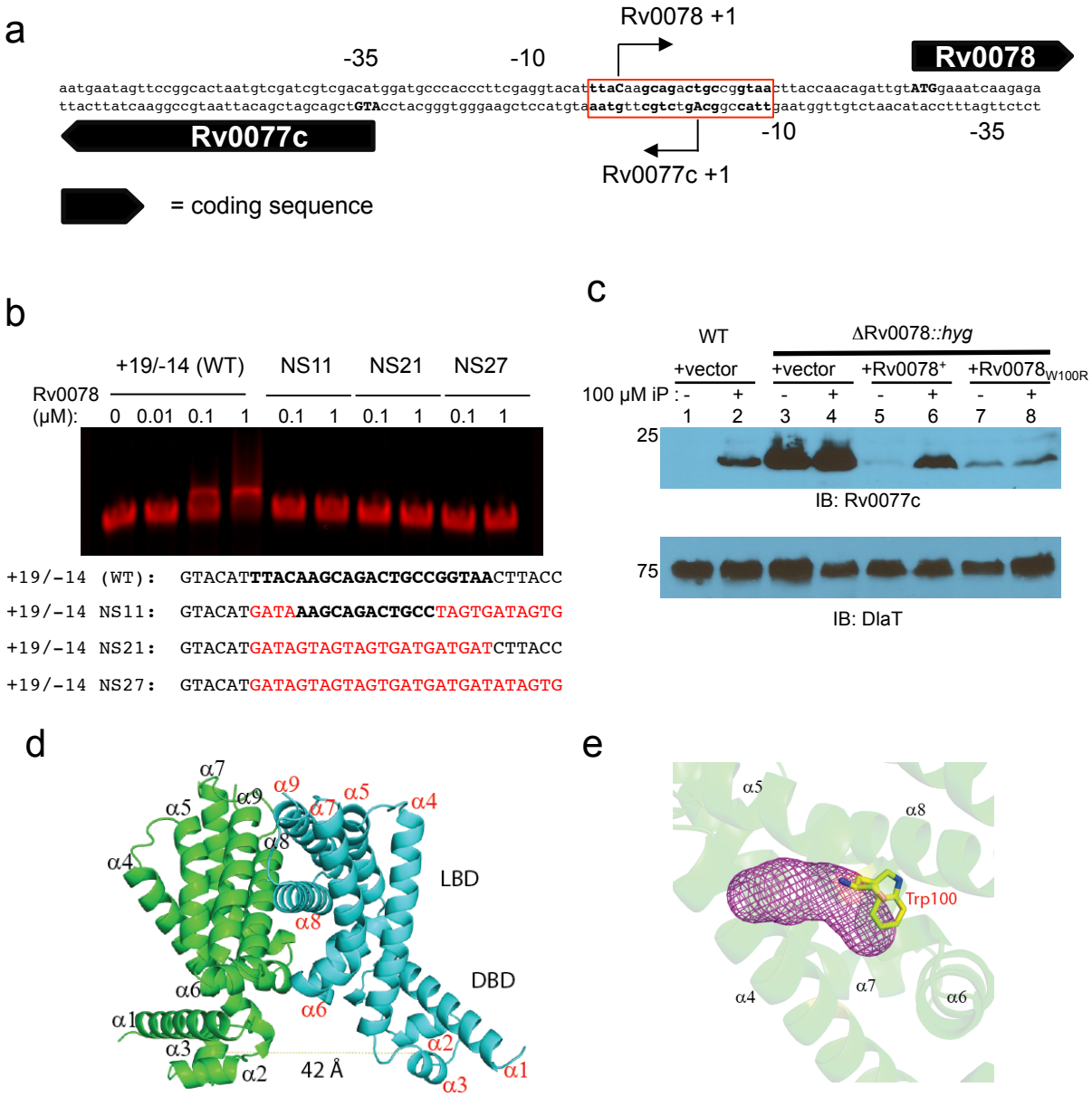

Figure 2. Rv0078 represses the expression of Rv0077c. a, The putative transcriptional start sites (+1) of Rv0077c and Rv0078 as determined by 5'RACE (see Methods). The predicted start codons are in capital bold letters. **b,** EMSA analysis identifies a putative repressor binding site. Probe sequences. +19/-14 refers to positions relative to the Rv0077c +1. In bold is the presumed binding site. Mutated residues are in red. Not shown at the end of each probe is a sequence for annealing to a fluorescent tag (Supplementary Table S1). **c,** Deletion and disruption of Rv0078 results in the constitutive expression of Rv0077c. Total cell lysates were prepared and separated on a 10% SDS-PAGE gel. IB = immunoblot. The membrane was stripped and incubated them with antibodies to DlaT to confirm equal loading of samples. Molecular weight standards are indicated to the left of the blots and are in kilodaltons (kD). **d**, A cartoon view of the crystal structure of the apo Rv0078 dimer at 1.85 Å resolution (PDB 5WM9). LBD, ligand binding domain. DBD, DNA binding domain. e, The purple mesh shows a putative ligand binding pocket surrounded by helices α4 to α8 in the LBD of one Rv0078 monomer. Trp100, which was required for cytokinin-dependent induction, is labeled.

Samanovic et al, Figure 3

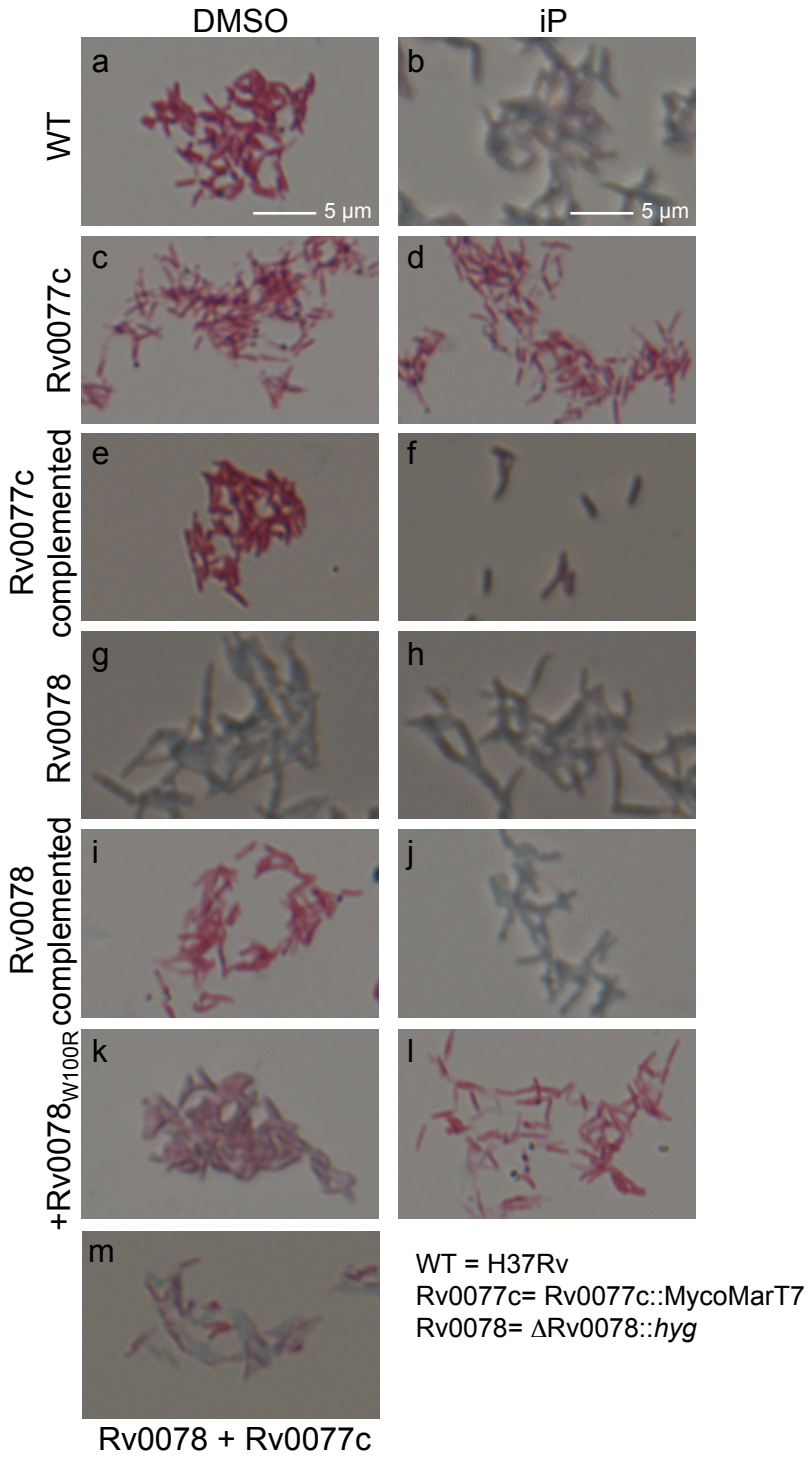

Figure 3. Induction of Rv0077c expression results in loss of acid-fast staining. *M. tuberculosis* strains were examined by Ziehl-Neelsen staining. Magnification is 63-fold. Scale bars are applicable to all images. See text for details.

Samanovic et al, Figure 4

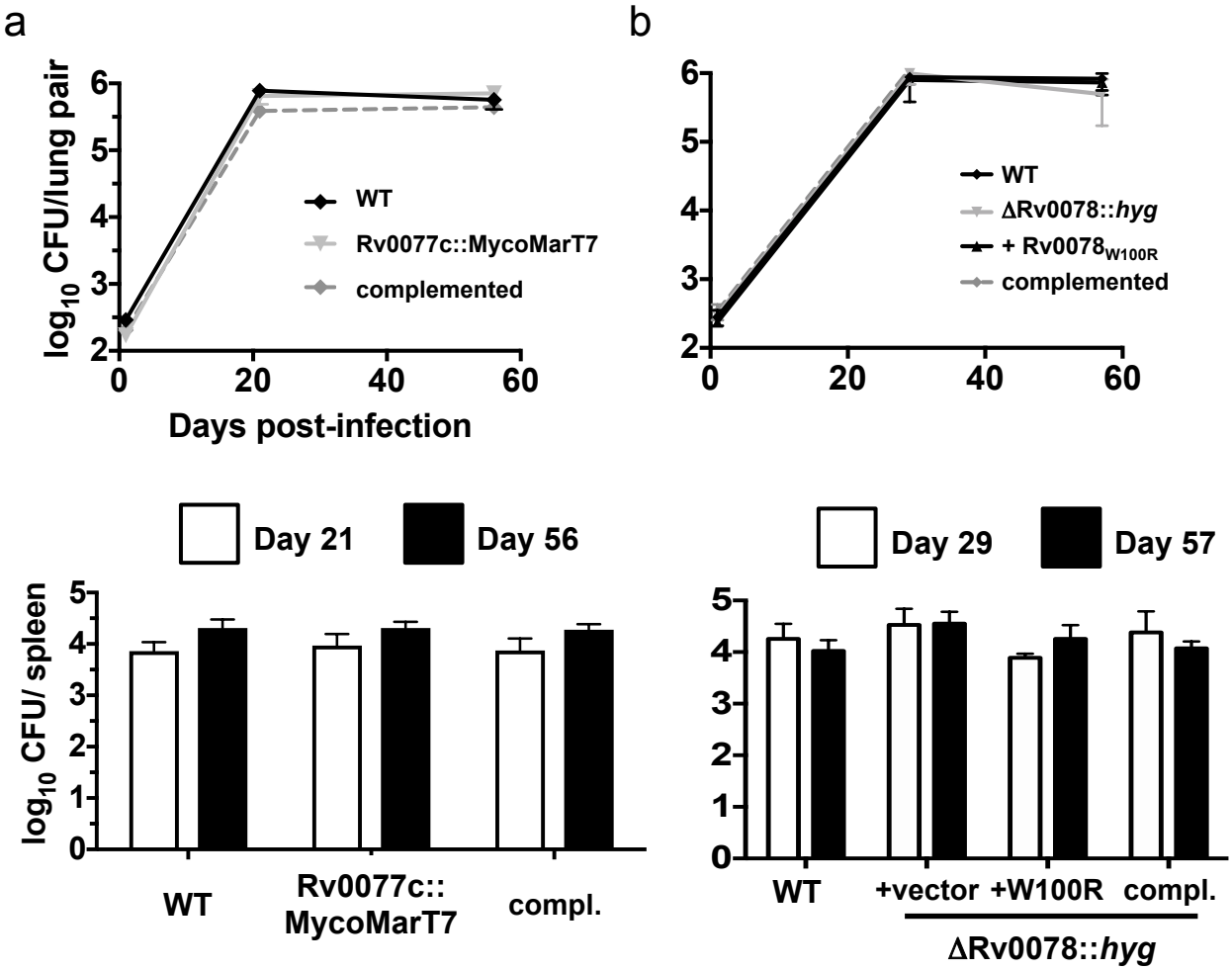

Figure 4. Loss of Rv0077c or Rv0078 does not attenuate bacterial survival in mice. **a,** Bacterial colony forming units (CFU) after infection of C57BL/6J mice with WT, Rv0077c and complemented strains. **b,** Bacterial CFU after infection of C57BL/6J mice with WT, Rv0078 and complemented strains. For both panels, data in each are from a single experiment that is representative of two independent experiments. Error bars indicate the standard error of the mean.